

CHAPTER IV

RESULTS AND DISCUSSION

4.1 Extended Hildebrand Solubility Parameter Group Contribution

According to the previous work, Roughton *et al.* (2012) proposed the group contribution solubility parameter model for ILs (δ_{IL}) as shown in equation (4.1) which was used to predict the solubility parameter s at 298.15 K.

$$\begin{aligned}\delta_{IL} &= \delta_{\text{Alkyl chain}}^C + \delta_{\text{Cation}}^C + \delta_{\text{Anion}}^C \\ &= \sum_{\text{Alkyl chain}} n_i C_i + \sum_{\text{Cation}} n_j C_j + \sum_{\text{Anion}} n_k C_k + b\end{aligned}\quad (4.1)$$

Where, subscript i , j , and k represent alkyl chain groups, cation groups, and anion groups respectively. n_i describes the number of groups of type i , C_i is the contribution of group i to the overall solubility parameter value, and b is a constant value.

In this work, the Hildebrand solubility parameter group contributions (GC) of ILs are extended. Experimental values for 39 different ILs at 298.15 K were used for the development of the Hildebrand solubility parameter GC model (Marciniak, 2010, Marciniak, 2011, Weerachanchai *et al.*, 2012, Yoo *et al.*, 2012). These ILs can be broken down into 5 alkyl chains, 8 cations and 20 anions groups and were used to describe the ILs in the data set. The contribution parameters for each group are given in Table 4.1. The total numbers of independent variables in the model are 34 (including a constant term). The developed model (see equation 4.1) provides a good fit of experimental data with a value of 0.319%AARD (percent average absolute relative deviation) between the predicted and experimental solubility parameter values as shown in Figure 4.1 (see more calculation details in Appendix A). The maximum relative deviation observed was 3.29. For example, 1-Ethyl-3-methylimidazolium tetrafluoroborate, [C₂mim][BF₄], consists of 2 CH₃ groups (i), 1 CH₂ group (i), 1 Imidazolium [Im] cation group (j), and 1 Tetrafluoroborate [BF₄]

anion group (k). By using Equation 4.1 and Table 4.1, the solubility parameter of $[\text{C}_2\text{mim}][\text{BF}_4]$ is $32.07 \text{ MPa}^{1/2}$.

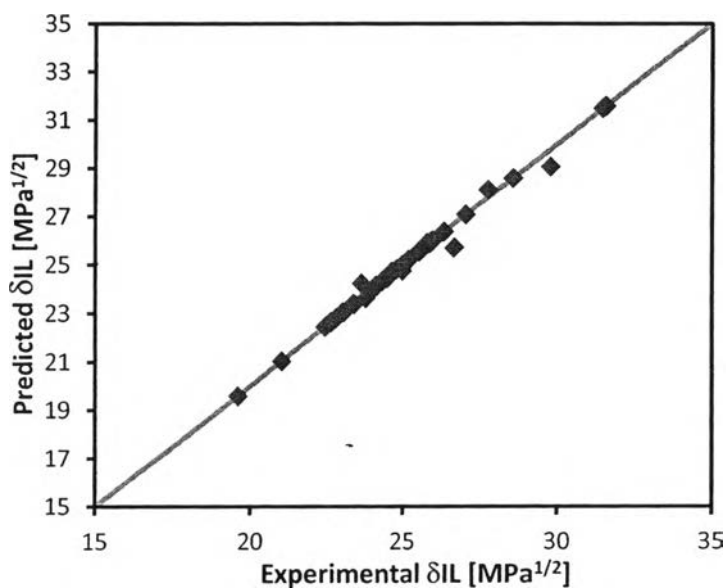


Figure 4.1 Comparison between experimental and predicted solubility parameter values.

Table 4.1 Extended GC values for ILs Hildebrand solubility parameter model

	Ionic Liquid groups	C_i [$\text{MPa}^{1/2}$]
Alkyl chain group (i)	CH_3	1.28
	CH_2	-0.24
	CH	-0.04
	CH_2O	-2.22
	OH	3.04
Cation groups (j)	Imidazolium [Im]	5.14
	Pyridinium [Py]	4.95
	Pyrrolidonium [Pyr]	5.31
	Phosphonium [P]	-0.05

Table 4.1 Extended GC values for ILs Hildebrand solubility parameter model
(Continued)

	Ionic Liquid groups	Ci [MPa^{1/2}]
	Sulfonium [S]	-0.79
	Piperidinium [Pip]	2.84
	Ammonium [A]	3.32
	Isoquinolinium [Isoq]	4.16
Anion groups (k)	Trifluoroacetate [CF ₃ COO]	0.62
	Thiocyanide [SCN]	0.25
	Trifluoromethane sulfonate [CF ₃ SO ₃]	-1.81
	2-(2-Methoxyethoxy)ethyl sulfate [MDEGSO ₄]	0.33
	Octyl sulfat [OcSO ₄]	0.33
	Tosylate [TOS]	-1.22
	Bis(trifluoromethylsulfonyl)imide [Tf ₂ N]	1.24
	Dimethyl phosphate [DMP]	1.9
	Diethyl phosphate [DEP]	1.01
	Tetrafluoroborate [BF ₄]	7.13
	Hexafluorophosphate [PF ₆]	4.61
	Chloride [Cl]	-0.33
	Acetate [Ac]	0.22
	Dicyanamide [N(CN) ₂]	0.9
	Nitrate [NO ₃]	3.32
	[MeSO ₄]	1.18
	Ethylsulfate [EtSO ₄]	-0.49
	Methylsulfate [TCB]	0.96
	Trifluorotris(perfluoroethyl)phosphate [FAP]	0.24
	Hexafluoroantimonate [SbF ₆]	7.03
Constant value	b	17.48

4.2 A Systematic Methodology for the Screening of ILs as Entrainers and the Design of ILs-Based Separation Processes

A systematic methodology for the screening of ILs as entrainers and for the design of ILs-based separation processes in various homogeneous binary azeotropic mixtures has been developed. The overall methodology is presented in Figure 4.2.

The methodology of this work consists of four main steps (Figure 4.2). Step-1 is dedicated to the stability of the ILs by considering their chemical stability (hydrolysis) and thermal stability (thermal decomposition). The information of the stability of the ILs was collected from literature search. Step-2 is dedicated to the miscibility of the ILs and the target component, the main concept of miscibility between ILs and target component can be summarized as shown in Figure 4.3. The target solute component was considered as a key target property to further screen the candidates through the plot between the mole fraction of the ILs in the target component and the solubility parameter of the ILs as illustrated in Figure 4.4 and Figure 4.5. From this step the best candidates for aqueous systems and non-aqueous systems have been found. Step-3 is dedicated to the design and simulation of separation feasibility and energy requirement based on minimum energy requirement. The best candidates for aqueous systems (no more than 5 ILs) were used as entrainers, and then an extractive distillation column (EDC) and ILs recovery column were designed and simulated with the Pro/II 9.1 (PRO II User's Guide, 2006) simulator to determine the overall energy consumption of the ILs-based separation processes. The Non Random Two Liquids (NRTL) thermodynamic model (Renon and Prausnitz, 1968) was used to predict the vapor-liquid equilibrium of the ternary systems containing selected ILs by using Integrated Computer Aided System, ICAS—utility toolbox (Gani, 2006). Step-4 is dedicated to the modification of the separation process to obtain design flexibility for other azeotropic series, for aqueous systems, the isopropanol + water azeotropic mixture was investigated. The fixed variable was kept as the ethanol + water separation (the same ionic liquid entrainer and product purity). The design flexibility such as reflux ratio (RR), number of stages (N_s), feed stage location (N_f), and ILs flowrate have been investigated with

respect to the change in size of the alcohol, for instance, ethanol ($\text{CH}_3\text{CH}_2\text{OH}$), and isopropanol ($\text{CH}_3\text{CH}_2\text{CH}_2\text{OH}$).

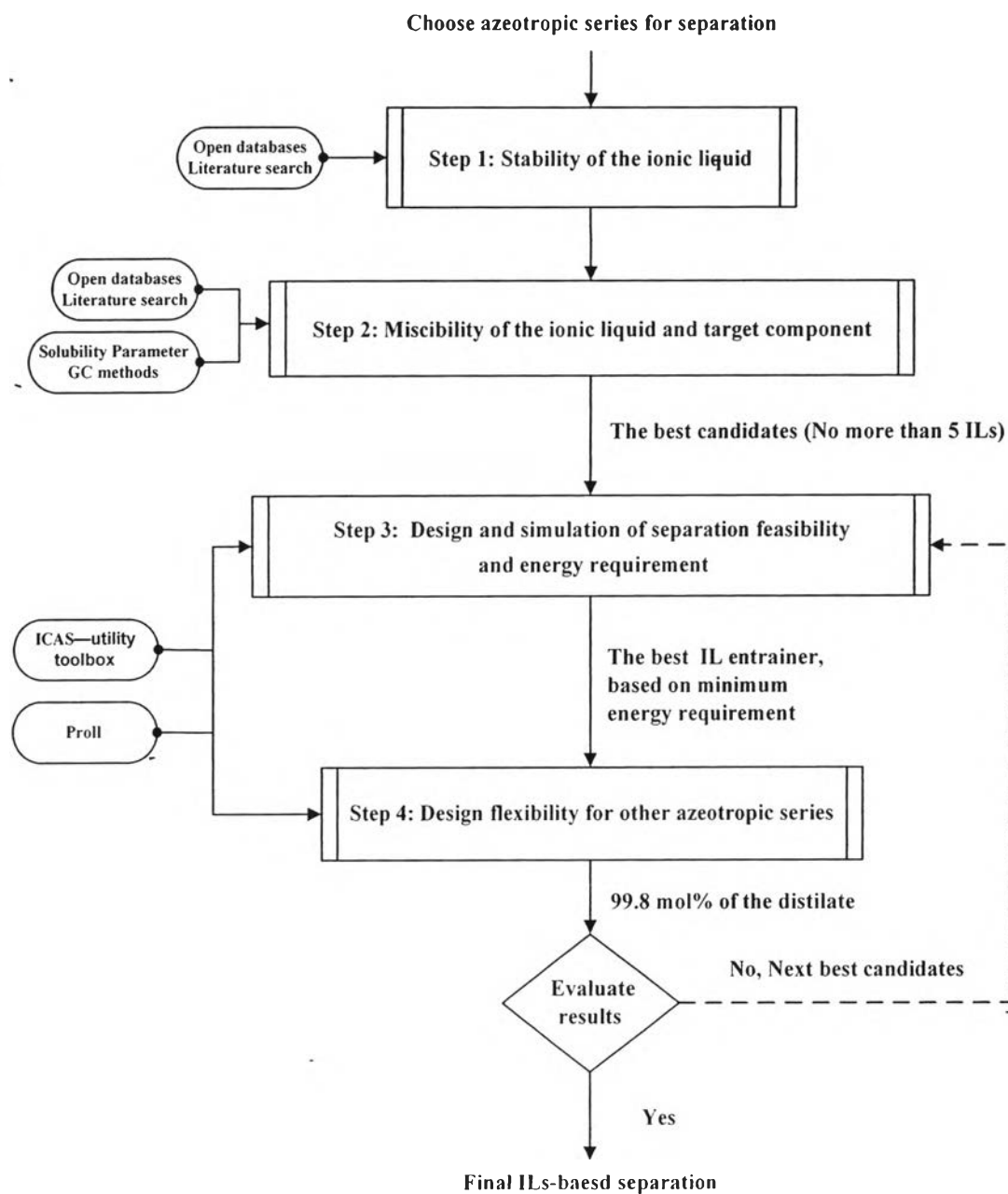


Figure 4.2 Overall methodology for the screening of ILs and for the design of ILs-based separation processes.

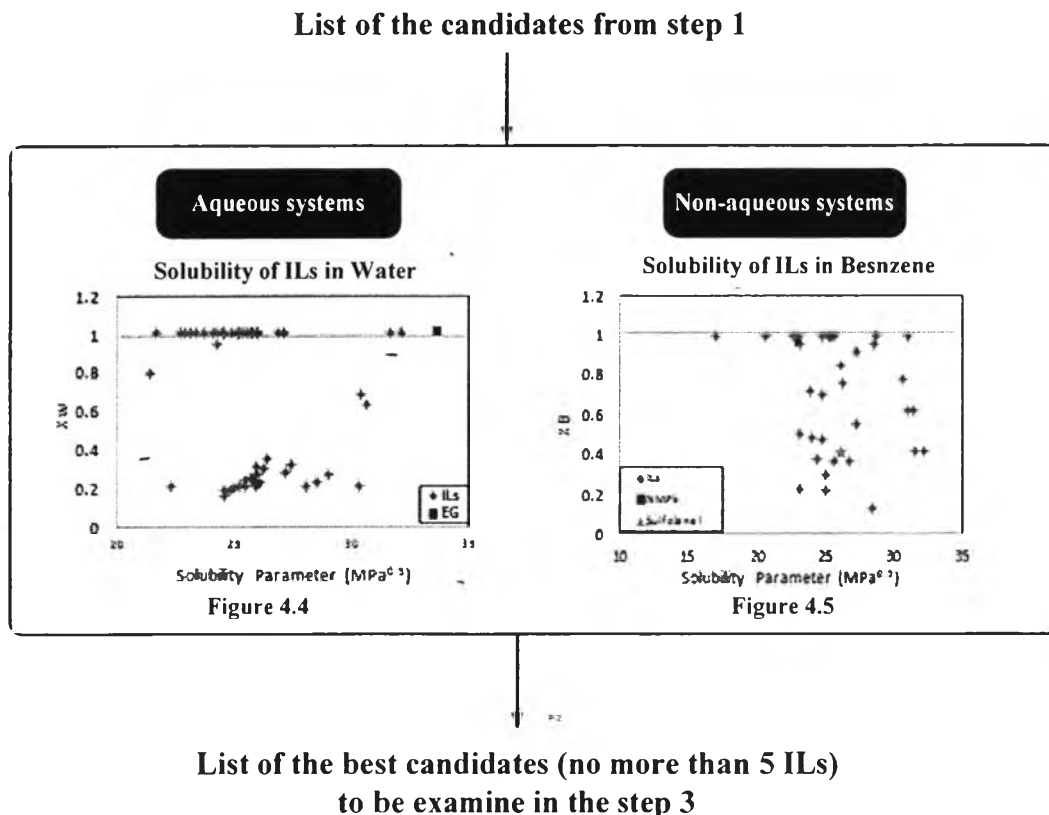


Figure 4.3 Summary of the miscibility between ILs and target component screening concept (step 2).

4.2.1 Step-1 : Stability of the Ionic Liquid

With regard to the environmental stability, the hydrolytic stability and thermal stability of ILs are considered first. From the literature search, the stability of the ILs strongly depends on the anions. Typical ILs consist of halogen-containing anions such as $[\text{AlCl}_4]$, $[\text{PF}_6]$, $[\text{BF}_4]$, $[\text{CF}_3\text{SO}_3]$ or $[(\text{CF}_3\text{SO}_2)_2\text{N}]$, which in some regard limits their ‘greenness’. The presence of halogen atoms may cause serious concerns if the hydrolytic stability of the anion is poor (e.g., for $[\text{AlCl}_4]$ and $[\text{PF}_6]$) or if a thermal treatment of spent ILs is required. In both cases, additional effort is needed to avoid the liberation of toxic and corrosive hydrofluoric acid (HF) or hydrochloric acid (HCl) into the environment (Sowmia et al., 2009). Freire et al. (2009) indicated that the use of ILs based on Tetrafluoroborate $[\text{PF}_6]^-$ and Hexafluorophosphate $[\text{BF}_4]^-$ anions can hydrolyze in water and at high temperature

they lead to the formation of HF—very toxic and corrosive compound. With increasing length of the alkyl chain, the extent of the anion hydrolysis is increased.

In term of thermal stability of ILs, decomposition temperature (T_d) depends on the type of cation. For example, the imidazolium-based ILs appear to have a better thermal stability than the pyridinium-based and tetraalkylammonium-based ILs (Lazzús, 2012). In general, remarkable differences in T_d are observed by changing the anions, a simple extension of alkyl chain hardly affects the T_d in imidazolium cation. Comparing the anions, ILs composed of BF_4 , PF_6 , and Tf_2N are thermally more stable than corresponding halides (I, Br, Cl). The relative anion stability follows the order: $\text{PF}_6 > \text{BF}_4 > \text{AsF}_6 \gg \text{I, Br, Cl}$ (Sowmiah et al., 2009).

Therefore, ILs as entrainers should consist of imidazolium-based cations and non-halogen containing anions with respect to the stability of ILs

4.2.2 Step-2 : Miscibility of the Ionic Liquid and Target Component

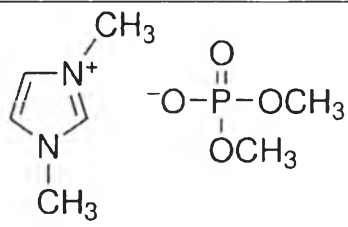
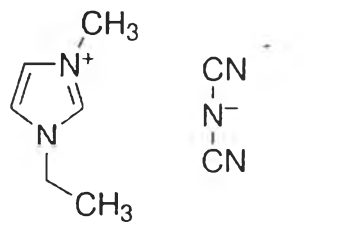
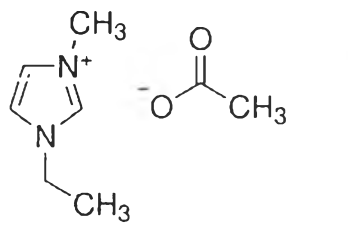
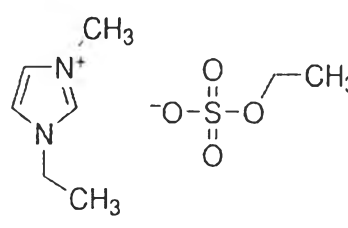
The concept of miscibility between ILs and target component can be summarized in Figure 4.3. The miscibility of the ILs and the target component was plotted against the Hildebrand solubility parameter as illustrated in Figure 4.4 and Figure 4.5. The Hildebrand solubility parameter GC model was required to predict the solubility parameter of the ILs.

4.2.2.1 Aqueous Systems

Solubility of ILs in water expressed as a function of the solubility parameters of the ILs was illustrated in Figure 4.4. The mole fraction of ILs in water was obtained from the literature (see more in Appendix B) and the solubility parameter of the ILs was calculated from the Hildebrand solubility parameter GC (equation 4.1). To avoid phase splitting of liquid mixtures, the best suitable entrainers should have a solubility parameter close to or similar to the solubility parameter of water as the target component and be completely miscible with water. For water as the target component, the solubility parameter of water is $48 \text{ MPa}^{1/2}$ (Barton, 1991). The closest ILs are 1-ethyl-3-methylimidazolium tetrafluoroborate, $[\text{C}_2\text{mim}][\text{BF}_4]$ ($\delta_{\text{IL}} = 32.07 \text{ MPa}^{1/2}$) and 1-butyl-3-methylimidazolium tetrafluoroborate, $[\text{C}_4\text{mim}][\text{BF}_4]$ ($\delta_{\text{IL}} = 31.60 \text{ MPa}^{1/2}$). However, due to the stability limitation, these two ILs can form a hydrolysis in water and cause the formation of HF. Hence, they are not suitable as

entrainers. The criteria for screening suitable ILs are 1) completely miscible with water, and 2) non-halogen containing anions. Finally, four ILs, which are 1-ethyl-3-methylimidazolium ethylsulfate $[C_2MIM][EtSO_4]$, 1,3-dimethylimidazolium dimethyl phosphate $[C_1MIM][DMP]$, 1-ethyl-3-methylimidazolium acetate $[C_2MIM][Ac]$, and 1-ethyl-3-methylimidazolium dicyanamide $[C_2MIM][N(CN)_2]$ were selected as best candidates for the aqueous systems. The chemical structure of these four best IL candidates is illustrated in Table 4.2.

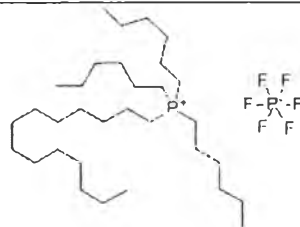
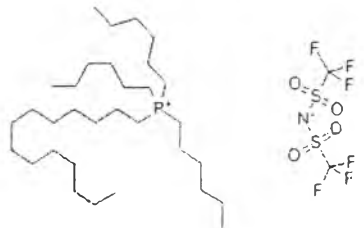
Table 4.2 Four best IL candidates for the aqueous systems (Step 2)

Ionic Liquids	Abbreviation	Chemical structure	$\delta_{IL}[MPa^{1/2}]$
1,3dimethyl imidazolium dimethyl phosphate	$[C_1MIM][DMP]$		27.08
1-ethyl-3- methylimidazolium dicyanamide	$[C_2MIM][N(CN)_2]$		25.84
1-ethyl-3- methylimidazolium acetate	$[C_2MIM][Ac]$		25.16
1-ethyl-3- methylimidazolium ethylsulfate	$[C_2MIM][EtSO_4]$		24.45

4.2.2.2 Non-aqueous Systems

For non-aqueous systems, benzene is considered as the target component with a solubility parameter of $18.7 \text{ MPa}^{1/2}$ (Barton, 1991). Figure 4.5 shows the mole fraction of the ILs in benzene as the target component is plotted against the Hildebrand solubility parameter GC (see more in Appendix B). The criteria for choosing the best candidates are the same as those considered in the aqueous systems. The best suitable entrainers should be closed to the solubility parameter of the target component and the mole fraction of ILs in benzene is equal to unity. The best two ILs with closest solubility parameter to benzene are Trihexyltetradecylphosphonium hexafluorophosphate $[\text{C}_6\text{C}_{14}\text{P}][\text{PF}_6]$ ($\delta_{\text{IL}} = 20.50 \text{ MPa}^{1/2}$) and Trihexyltetradecylphosphonium bis(trifluoromethylsulfonyl)imide $[\text{C}_6\text{C}_{14}\text{P}][\text{Tf}_2\text{N}]$ ($\delta_{\text{IL}} = 17.13 \text{ MPa}^{1/2}$). The chemical structures of these two best ILs candidates are illustrated in Table 4.3.

Table 4.3 Two best IL candidates for the non-aqueous systems (Step 2)

Ionic Liquids	Abbreviation	Chemical structure	$\delta_{\text{IL}}[\text{MPa}^{1/2}]$
Trihexyltetradecyl phosphonium hexafluorophosphate	$[\text{C}_6\text{C}_{14}\text{P}][\text{PF}_6]$		20.50
Trihexyltetradecyl phosphonium bis(trifluoromethylsulfonyl)imide	$[\text{C}_6\text{C}_{14}\text{P}][\text{Tf}_2\text{N}]$		17.13

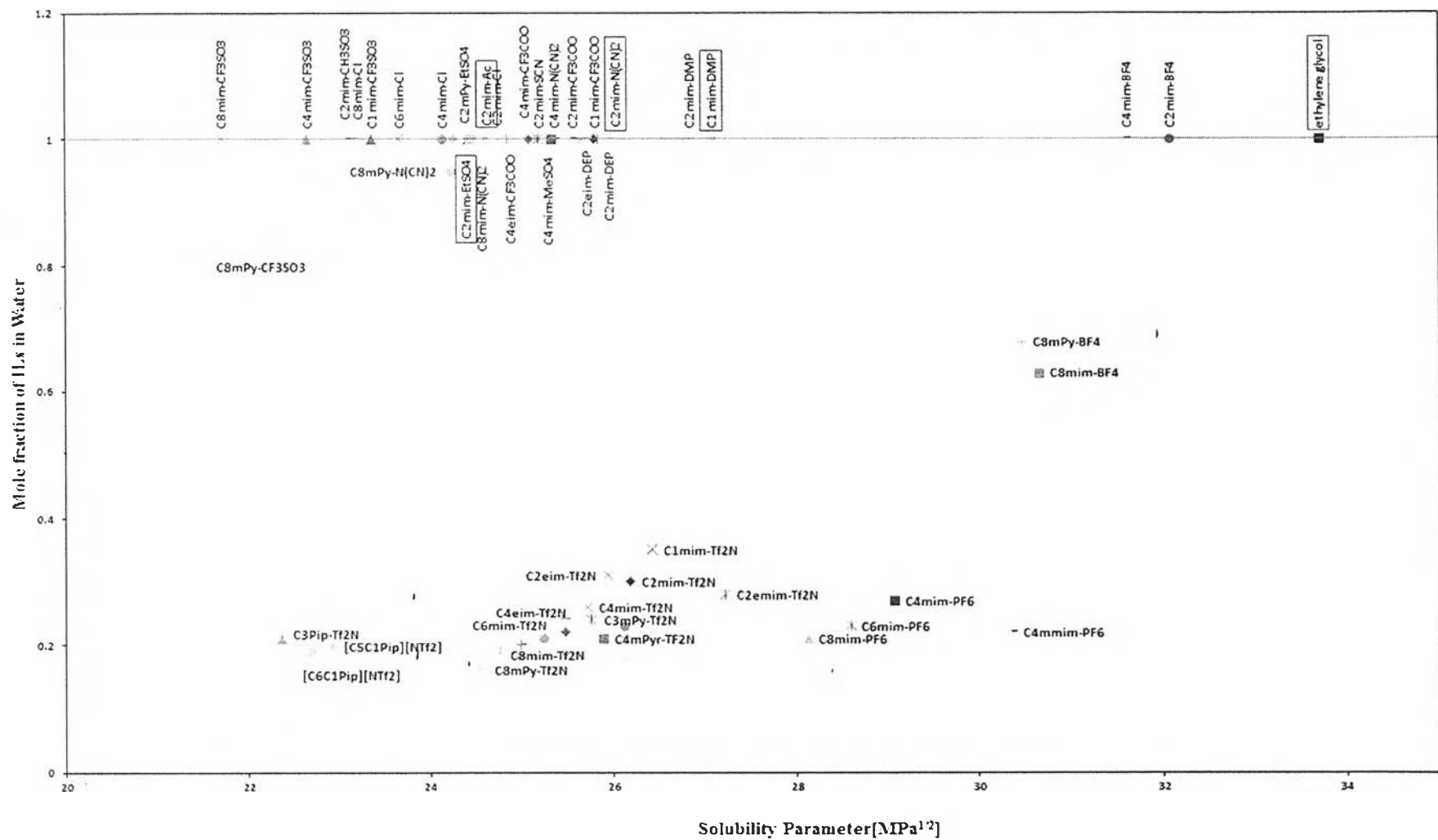


Figure 4.4 Solubility of ILs in water expressed as a function of the solubility parameters of the ILs.

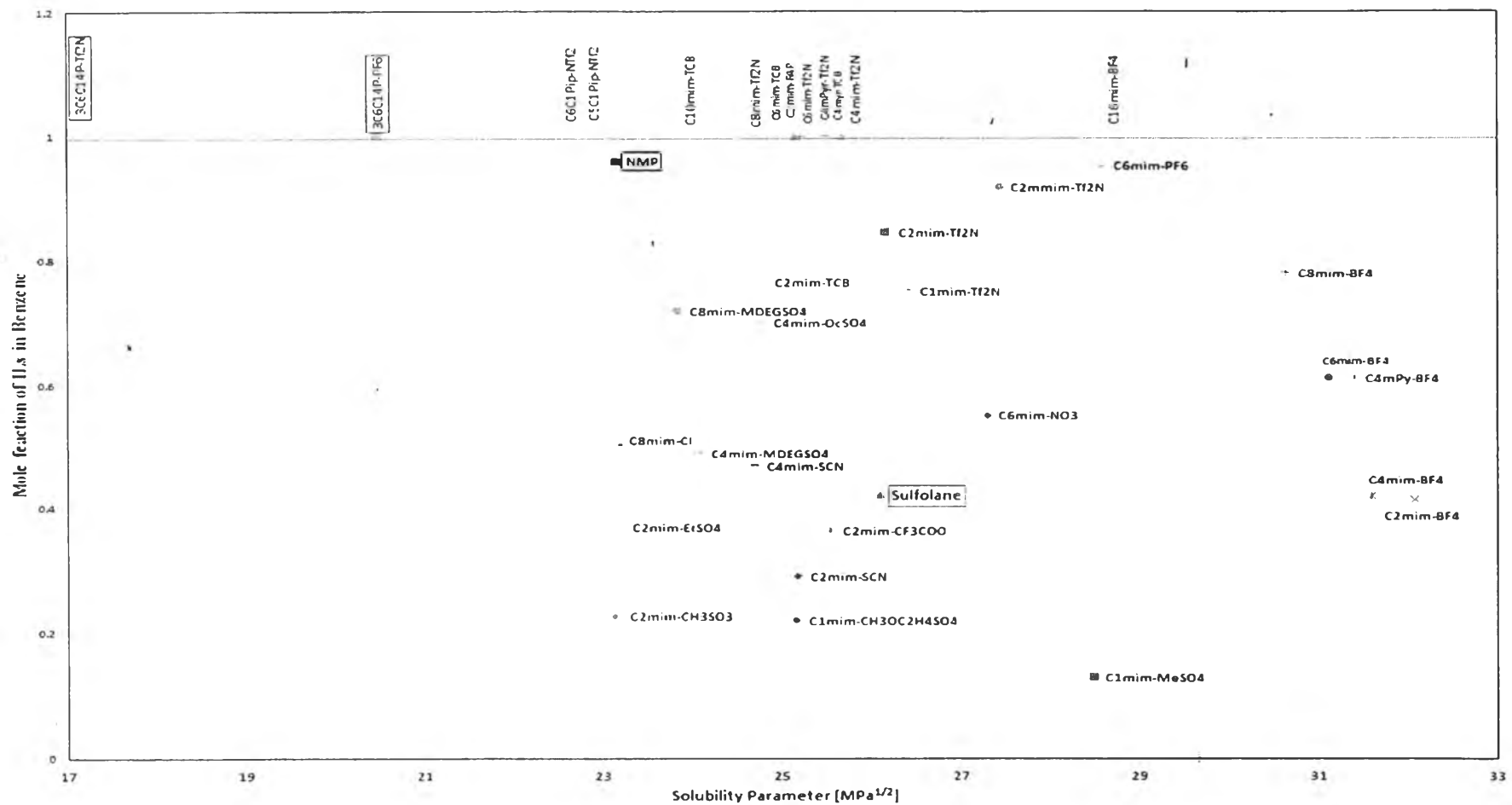


Figure 4.5 Solubility of ILs in benzene expressed as a function of the solubility parameters of the ILs.

4.2.3 Step-3 : Design and Simulation of Separation Feasibility and Energy

Requirement

Due to time limitation, only the aqueous systems have been evaluated through two case studies: ethanol + water and isopropanol + water. From the previous step, the best four candidates for aqueous systems were used as entrainers in a design and simulation of an extractive distillation column and an ILs recovery column to determine the optimal process for ILs-based separation of the homogeneous azeotropic systems

4.2.3.1 Property Models for Aqueous Systems

For design of ILs-based separation process, the ILs were model as alias component in the Pro/II simulator, using properties such as the liquid densities of the ILs (ρ_L), critical temperature (T_C), critical pressure (P_C), critical volume (V_C), normal boiling temperature (T_b), critical compressibility factor (Z_c), and acentric factor (ω) of ILs (Valderrama and Rojas, 2009) as shown in Appendix C (Table C1). The heat of vaporization for the volatile and their parameters for this equation were shown in Table C2 (Hernández, 2013). It should be noticed that due to the non-volatility of the ILs, their enthalpy of vaporization and vapor pressure were set as zero. The VLE of ternary systems containing ionic liquid was predicted by using NRTL thermodynamic model (Renon and Prausnitz, 1968), the binary interaction parameters and non-random factors were taken from available literatures (Zhao *et al.*, 2006, Calvar *et al.*, 2008, Hernández, 2013), (see more details in the Appendix C). The liquid enthalpy was estimated by Lee-Kesler (LK) method and the vapor enthalpy was predicted by the Soave-Redlich-Kwong equation of state (SRK).

4.2.3.2 Extractive Distillation Process Design for the Separation of Ethanol + Water Using Ethylene Glycol (EG)

The overall process for azeotropic mixtures separation processes using conventional solvent (EG) was performed by following the proposed design and simulation by Hernández (2013). The conventional extractive distillation process using ethylene glycol (EG) can be seen in Figure 4.6. The Fenske equation was used to calculate the minimum number of stages of the EDC, using the desired ethanol purity in the distillate and a relative volatility calculated at a solvent to feed

molar ratio of unity (arbitrary) at 100 kPa (Hernández, 2013). The actual number of stages for the EDC using EG was 30 (Hernández, 2013). The main feed was located at stage 23 (condenser at stage 1) and the solvent was fed at the 4th stage to avoid the solvent losses in the overhead of the column.

The solvent recovery column (SRC) was set to 15 actual stages and fed at the 8th stage. The overhead of the SRC was limited with the maximum EG fraction to less than 500 ppm to avoid solvent losses. As proposed by Hernández (2013), the pressure in the SRC was 20 kPa, provided a temperature in the condenser at 58 °C. The energy requirements for the whole ED process using EG as solvent are displayed in Table 4.6.

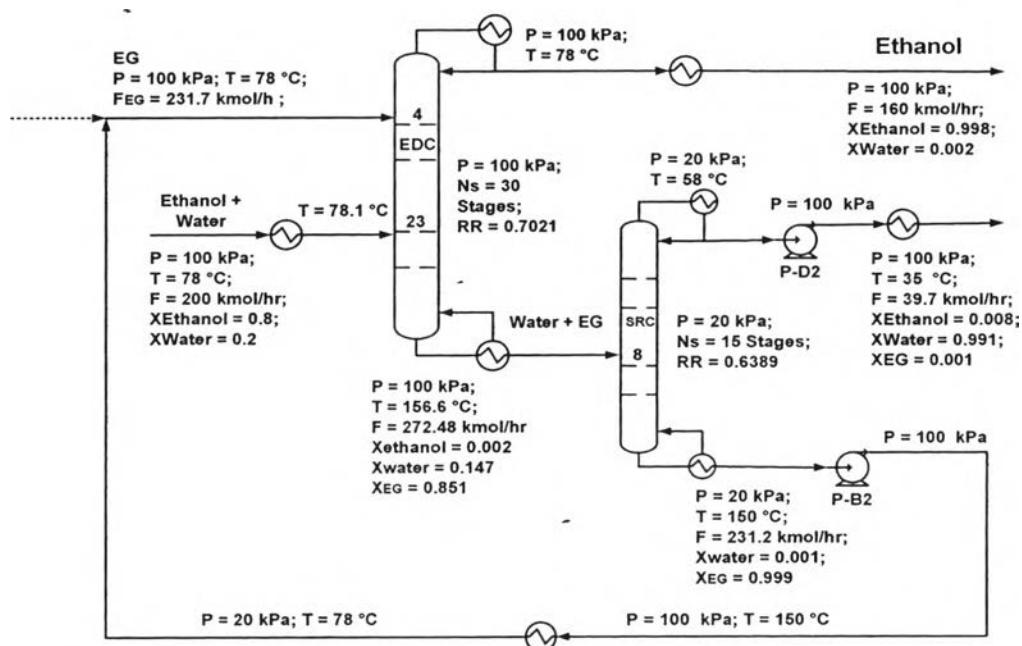


Figure 4.6 Conventional extractive distillation process using ethylene glycol (EG) (Hernández, 2013).

4.2.3.3 Extractive Distillation Process Design for the Separation of Ethanol + Water Using Four Best ILs Candidates

The separation processes using four best ILs candidates as entrainer for the ethanol + water mixture have been designed and simulated

successfully in literature (Seiler et al., 2004, Roughton et al., 2012). Based on representative plant capacities for bio-ethanol production (Seiler et al., 2004, Huang et al., 2008, Hernández, 2013), a saturated liquid of azeotropic mixture was fed at 200 kmol/h, which composed of 160 kmol/h of ethanol and 40 kmol/h of water at 100 kPa. The extractive distillation column was used to separate azeotropic mixture with a design specification of 160 kmol/h of distillate product at higher than 99.8 mol% ethanol purity. A pressure of 100 kPa was maintained throughout the system. The ILs recovery process was set to recover ILs at 99.8 mol%. Table 4.4 shows the overview of the fixed separation parameters and the process free variables to be optimized (Hernández, 2013).

In general, the entire separation process consists of a distillation column, a flash drum, and a stripper and the overview of the fixed separation parameters is illustrated in Figure 4.7. The extractive distillation column (EDC) is used to separate the light key component (ethanol) from the heavy key components (water and IL). The minimum number of theoretical stages of the EDC was set as 30 (Hernández, 2013), as calculated by using the Fenske equation using an arbitrary solvent to feed molar ratio of unity to obtain the relative volatility (Hernández, 2013). In the following section, a simple evaporation flash drum is used to remove any remaining ethanol from the water + IL due to the decrease in pressure to 10 kPa. The water + IL mixture is then sent to the stripper to separate the remaining water from the IL by using air at normal condition (25 °C and 100 kPa) to regenerate the desired IL with a molar purity of 0.998.

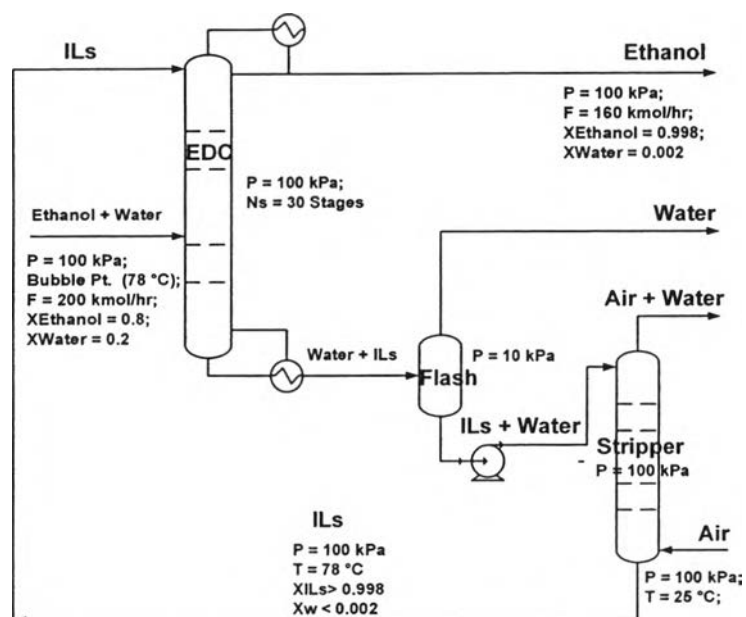


Figure 4.7 The process diagram of ILs-based azeotropic separation process (Seiler *et al.*, 2004, Roughton *et al.*, 2012).

The IL flowrate and the flash temperature were optimized by using the Pro/II optimizer to achieve the minimum overall energy requirements. The optimal feed stage location was determined by varying the feed stage to get the lowest the energy input in the reboiler. The minimum number of stages of the stripper was determined to satisfy the constraints of the final product purity of the IL entrainer leaving the stripping column (specified at 99.8% purity on a molar basis). The air flow rate was controlled by a controller to satisfy the constraints of the IL feed temperature to the EDC column (at the bubble point temperature of the water + ethanol feed stream, i.e. 78 °C).

For the aqueous systems, the four best IL candidates from section 4.2.2.1, which are $[C_2MIM][EtSO_4]$, $[C_1MIM][DMP]$, $[C_2MIM][Ac]$, and $[C_2MIM][N(CN)_2]$, were used as entrainers in the extractive distillation column. It is noted that the operating temperature of any stream in the process should be lower than the degradation temperature of each IL as shown in Table 4.5 in order to avoid its degradation.

Table 4.4 Separation task for ILs -based extractive distillation process

Fixed parameters		Process free variable
<i>Distillation column</i>		<i>Distillation column</i>
Operating pressure, kPa	100	Reflux ratio
Theoretical stages	30	Entrainer flow rate
<i>Column Feed</i>		Number of feed stages
Flow rate [kmol/h]	200	<i>Flash tank</i>
Xethanol	0.8	Temperature
Xwater	0.2	<i>Stripper</i>
Temperature	Boiling point	Number of stages
<i>Distillate</i>		Air flow rate
Flow rate [kmol/h]	160	
Xethanol	0.998	

Table 4.5 The degradation temperature of four best IL candidates

Ionic liquids	Degradation temperature (°C)	Reference
[C ₂ MIM][EtSO ₄]	251	Salgado <i>et al.</i> (2013)
[C ₁ MIM][DMP]	274	Salgado <i>et al.</i> (2013)
[C ₂ MIM][Ac]	160	Hernández (2013)
[C ₂ MIM][N(CN) ₂]	240	Paraknowitsch <i>et al.</i> (2010)

The input variables and the simulation results are summarized in Table 4.6. The separation process flowsheet, the stream tables, and overview of temperature, flowrate, separation factors, liquid fractions of all components in the extractive distillation process are shown in Appendix D for all simulation processes. The feed stage location of the EDC was found by the minimum energy consumption of the reboiler heat duty (see in Appendix D).

It was mentioned by Hernández (2013) for the separation of ethanol + water using $[\text{C}_2\text{MIM}][\text{Ac}]$ as entrainers, the EDC using $[\text{EMIM}][\text{OAc}]$ cannot be operated at 100 kPa because the bottom temperature reached 212.5 °C (higher than its degradation temperature). Therefore, to avoid the degradation of $[\text{C}_2\text{MIM}][\text{Ac}]$, the pressure in the extractive distillation column should be reduced to 25 kPa to get 152.36 °C at the bottom of EDC. For the $[\text{C}_2\text{MIM}][\text{Ac}]$ recovery section, it required extremely low pressures (1×10^{-7} kPa) to obtain the ionic liquid with a molar purity of 0.998 (Hernández, 2013). Therefore, the recovery column of $[\text{C}_2\text{MIM}][\text{Ac}]$ is not further discussed.

The optimal condition of the separation of ethanol + water using $[\text{C}_1\text{MIM}][\text{DMP}]$ is summarized in Figure 4.8. The theoretical stage of 28 was observed to recover isopropanol with a purity of 99.8 mol% at RR of 0.646. According to the results, the feed should be located at the 22th stage to obtain ethanol with a molar purity of 0.998. In the regeneration section, flash drum was operated at 182°C, and theoretical stage of 15 was required for the stripper column to get 99.8mol% of ILs.

Figure 4.9 shows the comparison of the reboiler heat duty of the extractive distillation column using different entrainers. It can be clearly concluded that the use of ILs as entrainers for separation of ethanol + water azeotrope can reduce around 9-20% of the reboiler duty in the extractive distillation column as compared to the conventional organic solvent (EG) (3.96 MW). Among all four IL candidates, $[\text{C}_1\text{MIM}][\text{DMP}]$ required the lowest reboiler duty (3.16 MW) due to its completely miscibility and relatively closest to the solubility parameter of water (see Figure 4.4), followed by $[\text{C}_2\text{MIM}][\text{N}(\text{CN})_2]$ (3.3 MW), $[\text{C}_2\text{MIM}][\text{EtSO}_4]$ (3.44 MW), and $[\text{C}_2\text{MIM}][\text{Ac}]$ (3.62 MW). Therefore, $[\text{C}_1\text{MIM}][\text{DMP}]$ can save reboiler energy consumption of 20.20 % (0.8 MW) when compared to the conventional solvent (EG).

Table 4.6 Input variables and the simulation results for ILs-based separation of the ethanol and water

	EG	[C2MIM][Ac]	[C ₂ MIM][N(CN) ₂]	[C ₂ MIM][EtSO ₄]	[C1MIM][DMP]
Entrainer flow rate, kmol/h	232.21	108.7	120	85	53.48
Main column					
Theoretical stages	30	30	30	30	30
Operating pressure, kPa	100	25	100	100	100
Ethanol purity	99.8 mol %	99.8 mol %	99.8 mol %	99.8 mol %	99.8 mol %
Reflux ratio	0.7021	0.9963	0.6128	0.8538	0.646
Entrainer feed stage	4	2	2	2	2
Ethanol + water feed stage	23	23	22	23	23
Bottom temperature, °C	156.16	152.36	170.3	174.88	170
Reboiler heat duty, MW	3.96	3.62	3.30	3.44	3.16
Entrainer regeneration					
Entrainer purity	>99.8 mol %	>99.8 mol %	>99.8 mol %	>99.8 mol %	>99.8 mol %
Distillation					
Theoretical stages	15	—	—	—	—
Operating pressure, kPa	100	—	—	—	—

Table 4.6 Input variables and the simulation results for ILs-based separation of the ethanol and water (Continued)

	EG	[C2MIM][Ac]	[C ₂ MIM][N(CN) ₂]	[C ₂ MIM][EtSO ₄]	[C1MIM][DMP]
Reflux ratio	0.6389	—	—	—	—
Feed stage	8	—	—	—	—
Reboiler heat duty, MW	0.681	—	—	—	—
Flash drum					
Operating pressure, kPa	—	—	10	10	10
Operating temperature, °C	—	—	200	251	182
Heat duty, MW	—	—	0.62	0.75	0.47
Stripping column					
Theoretical stages	—	—	10	10	15
Operating pressure, kPa	—	—	100	100	100
Feed stage	—	—	1	1	1
Bottom temperature, °C	—	—	78	78	78
Air flow rate, kg/h	—	—	8071	3798	2643
Air temperature, °C	—	—	25	25	25
Heat exchanger duty, MW	0.354	—	—	—	—
Overall heat duty, MW	4.64	—	3.92	4.20	3.64

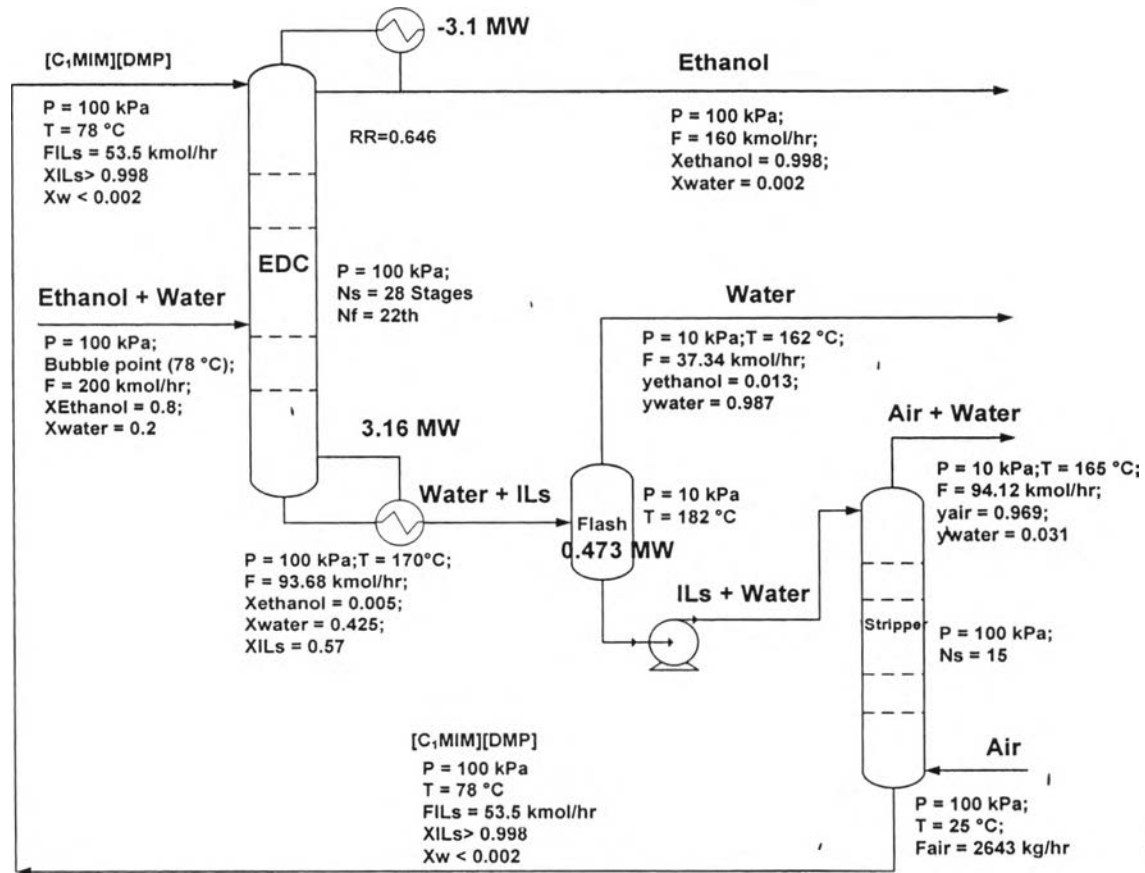


Figure 4.8 The optimal conditions and the results of the ethanol + water azeotropic separation processes using $[C_1MIM][DMP]$.

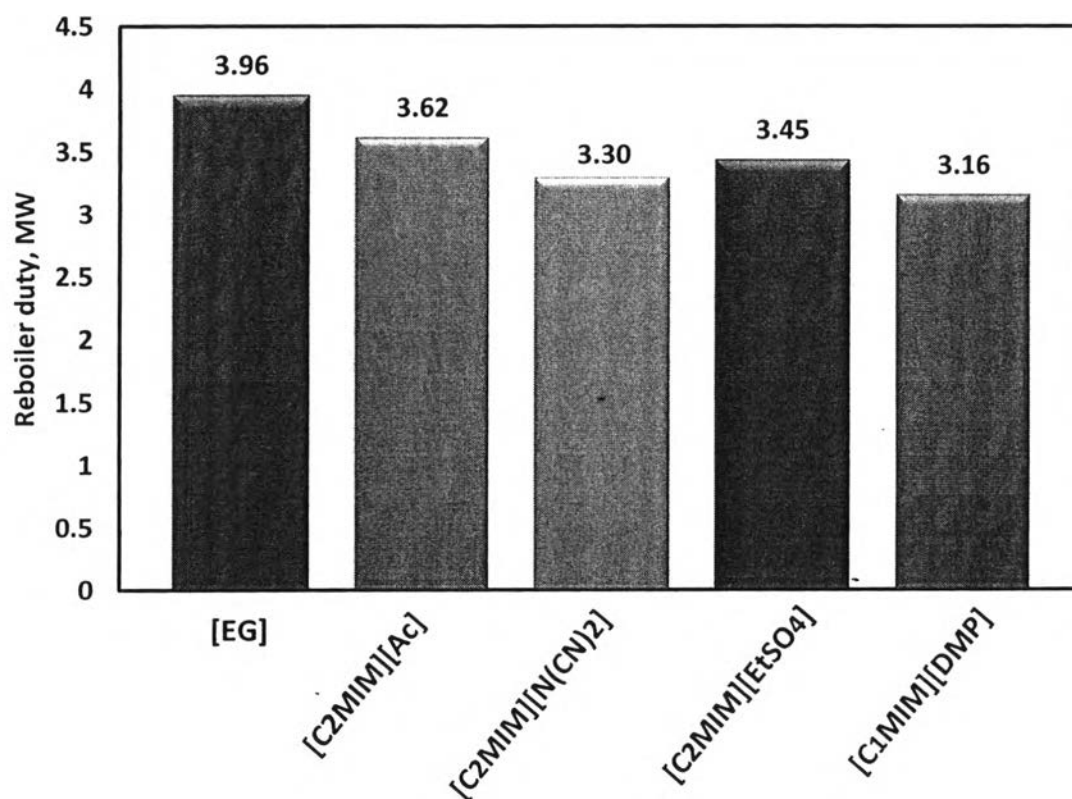


Figure 4.9 Energy requirement for reboiler in extractive distillation process using EG and four best IL candidates.

In term of ILs flowrate (Table 4.6), [C₁MIM][DMP] also requires the lowest flowrate (53.48 kmol/hr) for the breaking of the azeotrope as compared to other ILs. The liquid mole fraction of the [C₁MIM][DMP] profiles in each tray number of the extractive distillation process is shown in Figure D16 (Appendix D). From Figure D16, The liquid mole fraction of the [C₁MIM][DMP] in tray number 2 is 30 mol% and kept constant till tray number 22, then this fraction was dropped to 15 mol% of [C₁MIM][DMP]. This according to the VLE of the ethanol + water + [C₁mim][DMP] (see Figure C2) which the azeotrope was broken with a minimum of 10 mol% of [C₁MIM][DMP]. It should be noted that the adding the minimum requirement of ILs entrainer can reduce the material demands and improve the economics.

The overall energy requirement (reboiler duty plus recovery heat duty) for extractive distillation process using EG and different ILs entrainers is displayed in Figure 4.10. It can be obviously concluded that the use of $[C_1MIM][DMP]$ as entrainers provided the lowest in overall energy requirements and reduced the energy consumption by 21.55% compared to the conventional solvent (EG). The higher energy in the EG system is caused by the evaporation of EG in the reboiler, whereas the ILs are non-volatile. By comparing the overall energy consumption of each IL entrainer, the performance of the ILs for ethanol + water azeotropic system can be ranked as $[C_1MIM][DMP] > [C_2MIM][N(CN)_2] > [C_2MIM][EtSO_4]$. The $[C_1MIM][DMP]$ is chosen as the final candidate based on the minimum energy consumption of the whole processes.

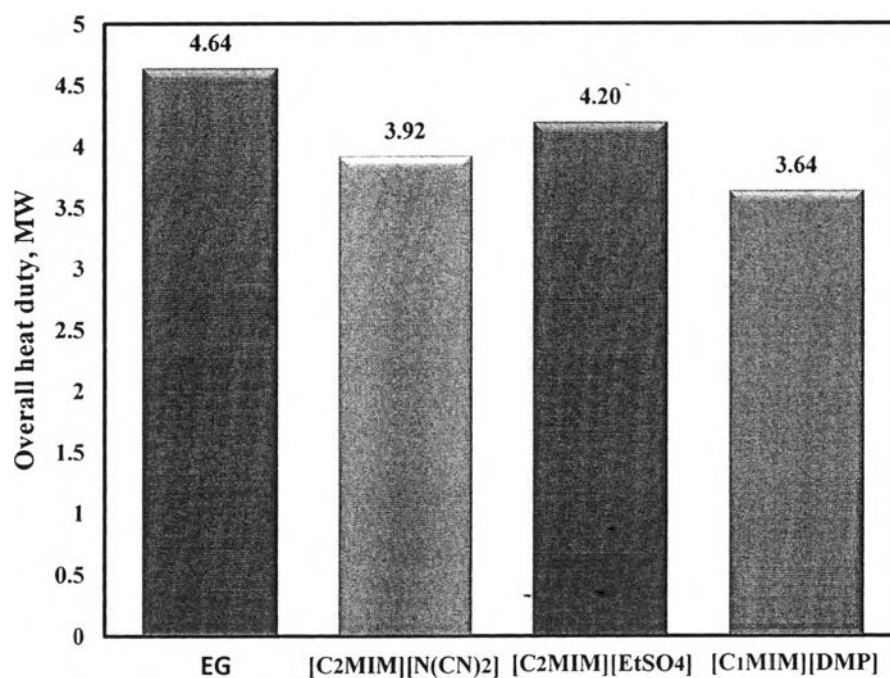


Figure 4.10 Overall energy requirement for extractive distillation process using EG and ILs.

4.2.4 Step-4 : Design Flexibility for Other Azeotropic Systems

The modification of the aqueous azeotropic separation process has been evaluated through the isopropanol + water azeotropic mixture (respect to the change in size of the alcohol). It should be noticed that the longer the carbon chain in an alcohol, the higher the non-polar properties of the mixtures is performed.

4.2.4.1 The Isopropanol + Water Separation Using $[C_1MIM][DMP]$

From the previous step, The $[C_1MIM][DMP]$ shows the best ILs entrainer for the ethanol + water separation. Thus, this IL has been selected to be used as an entrainer for the isopropanol + water separation. Figure 4.11 shows the result of the process simulation for the isopropanol + water separation using $[C_1MIM][DMP]$.

The separation of isopropanol + water using $[C_1MIM][DMP]$ required 43 number of stages which is higher than the ethanol + water separation (30 stages), and also required higher reboiler duty (7.045 MW) and higher reflux ratio (3.68) as compared to the separation of ethanol + water with the same IL entrainer. It can be noticed that in the recovery section, isopropanol (S2) can be recovered at a maximum molar purity of only 99.45 mol%, which is lower than the target purity (99.8 mol%). This according to the VLE diagram as illustrated in Figure 4.12 (b), The VLE diagram of isopropanol + water + $[C_1MIM][DMP]$ at 20 mol% of $[C_1MIM][DMP]$ shows closer to the diagonal line than those of ethanol + water + $[C_1MIM][DMP]$ at the same ILs concentration (Figure 4.12 (a)). Thus, it requires very large number of stage to obtain high product purity (99.8 mol%). To avoid this problem, the next best IL entrainer was selected from all best candidates ($[C_2MIM][N(CN)_2]$, $[C_2MIM][EtSO_4]$, or $[C_2MIM][Ac]$).

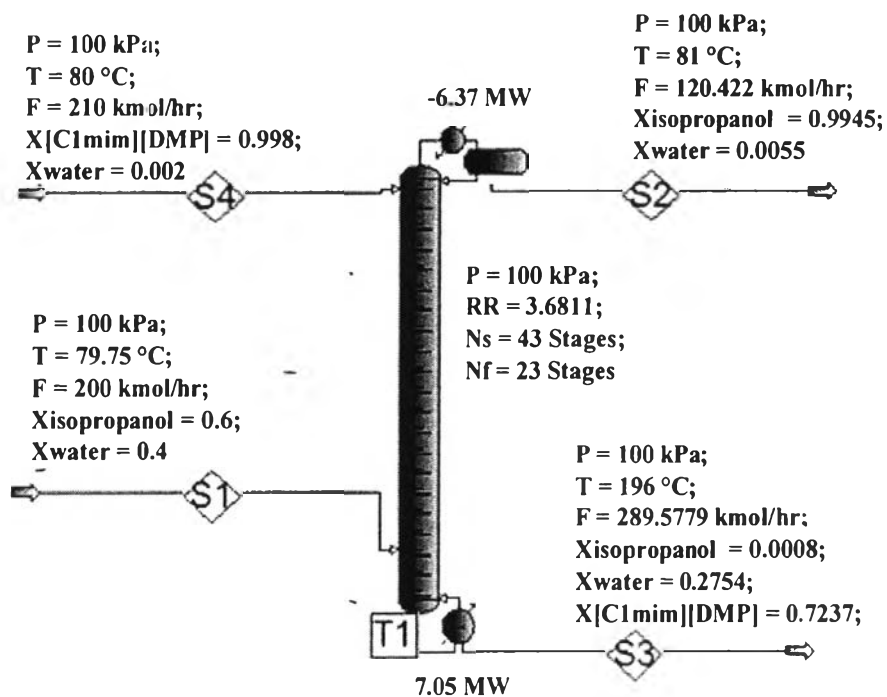
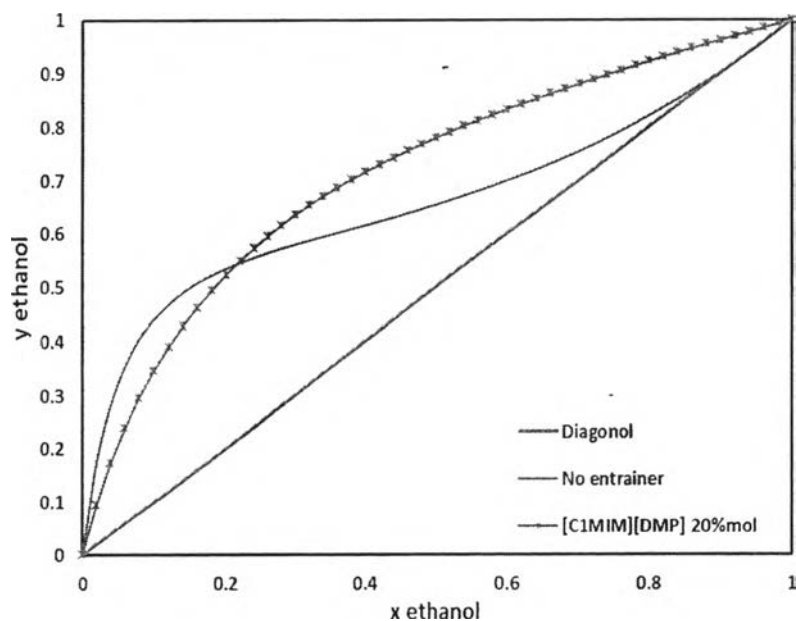
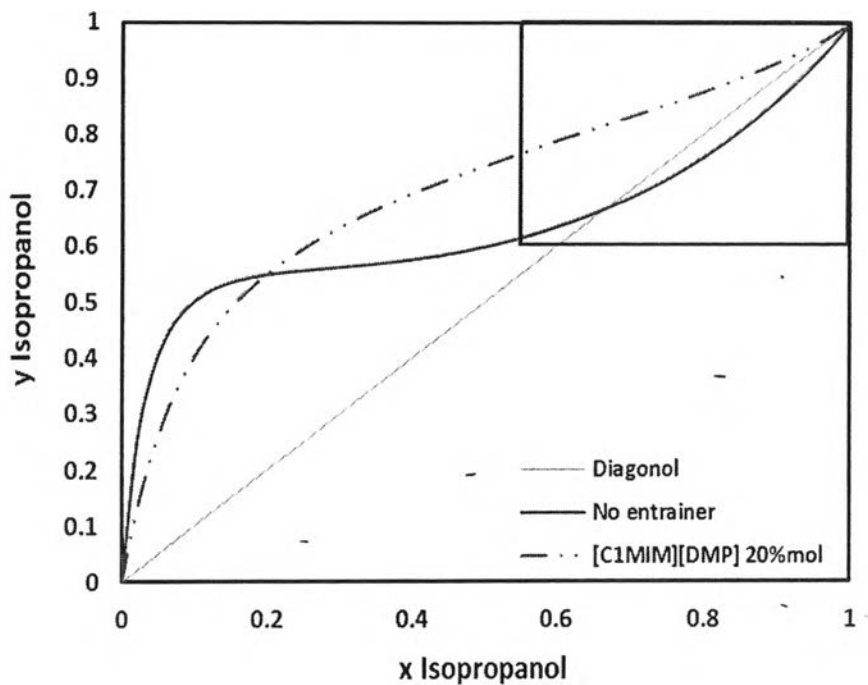


Figure 4.11 Extractive distillation column of isopropanol + water separation using $[\text{C}_1\text{MIM}][\text{DMP}]$.



(a)



(b)

Figure 4.12 VLE diagram of ethanol/water / $[C_1MIM][DMP]$ (a) and VLE diagram of isopropanol/water / $[C_1MIM][DMP]$ (b) at $[C_1MIM][DMP]$ 20%mol ($P = 1$ atm).

4.2.4.2 The Isopropanol+Water Separation Using $[C_2MIM][N(CN)_2]$

Due to the unfeasibility operation of the $[C_2MIM][Ac]$ (from the previous case; ethanol + water separation) and a lack of binary interaction parameters (NRTL) of $[C_2MIM][EtSO_4]$ for isopropanol + water separation, $[C_2MIM][N(CN)_2]$ was the only next best candidate to be used as entrainer for the isopropanol + water separation. The VLE diagram of isopropanol + water + $[C_2MIM][N(CN)_2]$ at different concentration of IL at $P = 1$ atm is shown in Figure C6. The NRTL interaction parameters for the ternary system were taken from Wang et al. (2010).

An analogous procedure of the ethanol + water using $[C_2MIM][N(CN)_2]$ separation process was applied for the separation of isopropanol + water. The separation process of the isopropanol + water is illustrated in Figure 4.13.

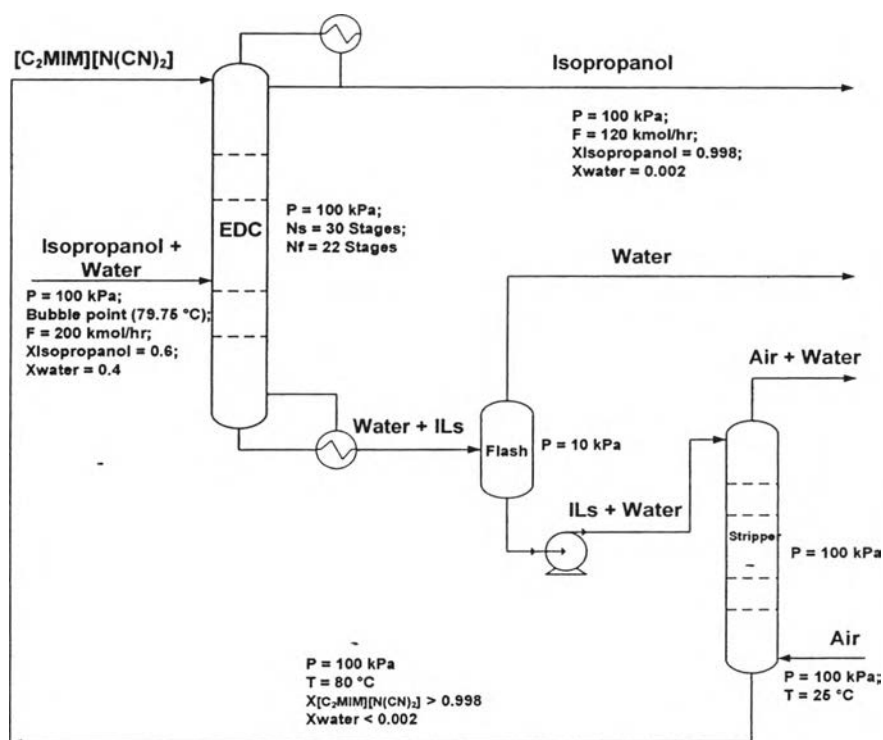


Figure 4.13 The process flow diagram of isopropanol + water azeotropic separation using $[C_2MIM][N(CN)_2]$.

4.2.4.2.1 The Change of the Heat Duty and Reflux Ratio in EDC

A comparison of simulation results between ethanol + water and isopropanol + water using $[C_2MIM][N(CN)_2]$ as entrainer is illustrated in Table 4.7. As can be seen from Table 4.7 and Figure 4.14, an increase of the size of the alcohol (ethanol $[CH_3CH_2OH]$ to isopropanol $[CH_3CH_2CH_2OH]$) for the EDC allows a slightly increase of the reflux ratio (from 0.6128 for ethanol to 0.729 for isopropanol), and a reduction of the reboiler heat duty as shown in Figure 4.14. It can be noticed that the interaction of the $[C_2MIM][N(CN)_2]$ and water for the isopropanol + water $[C_2MIM][N(CN)_2]$ system is stronger than that of the ethanol + water $[C_2MIM][N(CN)_2]$ system. This caused by the stronger interaction of the ethanol and water (higher polarity) than the isopropanol and water. Therefore, it is easier to recover isopropanol from water than recovering of ethanol from water and this leads to a lower energy consumption of the reboiler.

Considering the flash duty, due to the stronger interactions between $[\text{C}_2\text{MIM}][\text{N}(\text{CN})_2]$ and water in the isopropanol + water $[\text{C}_2\text{MIM}][\text{N}(\text{CN})_2]$ system, the recovery of the $[\text{C}_2\text{MIM}][\text{N}(\text{CN})_2]$ from water required the flash heat duty of 1.34 MW which is higher than that of the ethanol + water $[\text{C}_2\text{MIM}][\text{N}(\text{CN})_2]$ system (0.613 MW). Comparing the overall energy requirement, the isopropanol + water $[\text{C}_2\text{MIM}][\text{N}(\text{CN})_2]$ system require slightly lower energy than the separation of ethanol + water with the same IL and the same operating condition as shown in Figure 4.14.

Table 4.7 A comparison of the input variables and the simulation results for alcoholic aqueous azeotropic separation processes using $[\text{C}_2\text{MIM}][\text{N}(\text{CN})_2]$ when fixed condition as ethanol + water separation (Figure 4.8)

	Ethanol + water + [C₂MIM][N(CN)₂]	Isopropanol + water + [C₂MIM][N(CN)₂]
Entrainer flow rate, kmol/h	120	120
Main column		
Theoretical stages	30	30
Operating pressure, kPa	100	100
Ethanol purity	99.8 mol %	99.8 mol %
Reflux ratio	0.6128	0.729
Entrainer feed stage	2	2
Alcohol + water feed stage	22	22
Bottom temperature, °C	170.3	138.4
Reboiler heat duty, MW	3.300	2.54
Entrainer regeneration		
Entrainer purity	>99.8 mol %	>99.8 mol %
<i>Flash drum</i>		
Operating pressure, kPa	10	10
Operating temperature, C	200	200

Table 4.7 A comparison of the input variables and the simulation results for alcoholic aqueous azeotropic separation processes using $[\text{C}_2\text{MIM}][\text{N}(\text{CN})_2]$ when fixed condition as ethanol + water separation (Figure 4.8) (Cont'd)

	Ethanol + water + [C₂MIM][N(CN)₂]	Isopropanol + water + [C₂MIM][N(CN)₂]
Heat duty, MW	0.6181	1.3373
<i>Stripping column</i>		
Theoretical stages	10	10
Bottom temperature, °C	78	80
Air flow rate, kg/h	8071.1	8094
Air temperature, °C	25	25
Overall heat duty(Reboiler+Flash), MW	3.92	3.88

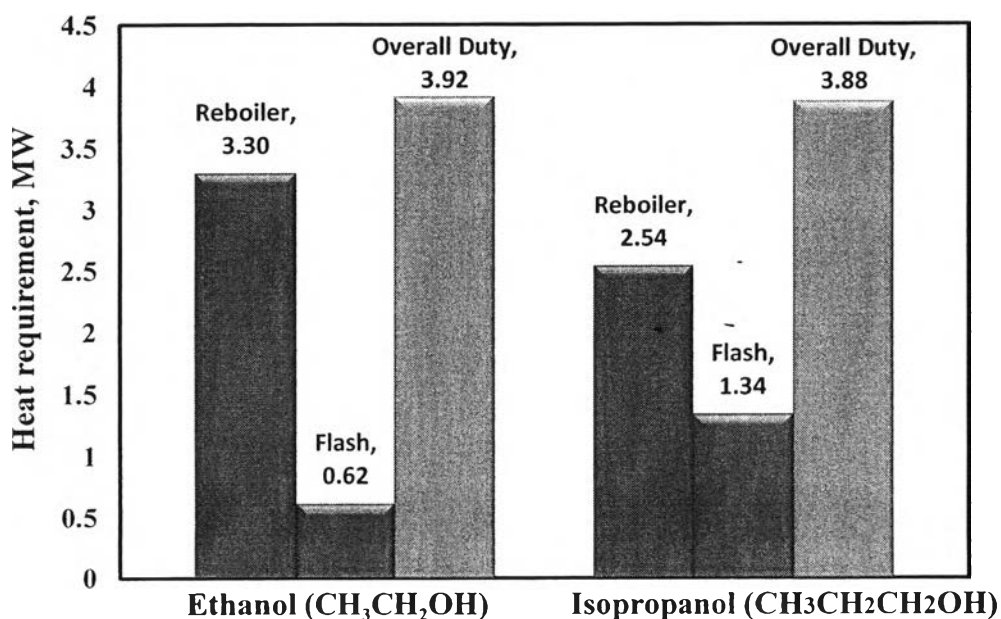


Figure 4.14 Heat requirement for the alcoholic + water azeotropic separation using $[\text{C}_2\text{MIM}][\text{N}(\text{CN})_2]$ as entrainer.

4.2.4.2.2 The Change of the Theoretical Stages in EDC

The optimal number of theoretical stages for the isopropanol + water separation with $[\text{C}_2\text{MIM}][\text{N}(\text{CN})_2]$ was investigated by given the reflux ration (RR) of 0.618 (as same as the ethanol + water + $[\text{C}_2\text{MIM}][\text{N}(\text{CN})_2]$ separation). The results are summarized in Figure 4.15. It can be seen that a maximum molar purity of the isopropanol was obtained from the number of theoretical stage 35-50 is 0.981, which does not satisfy the design criterion of 99.8 mol% purity of isopropanol. Thus, we cannot recover the isopropanol with higher purity than 98.1 mol%, at a fixed RR of 0.618.

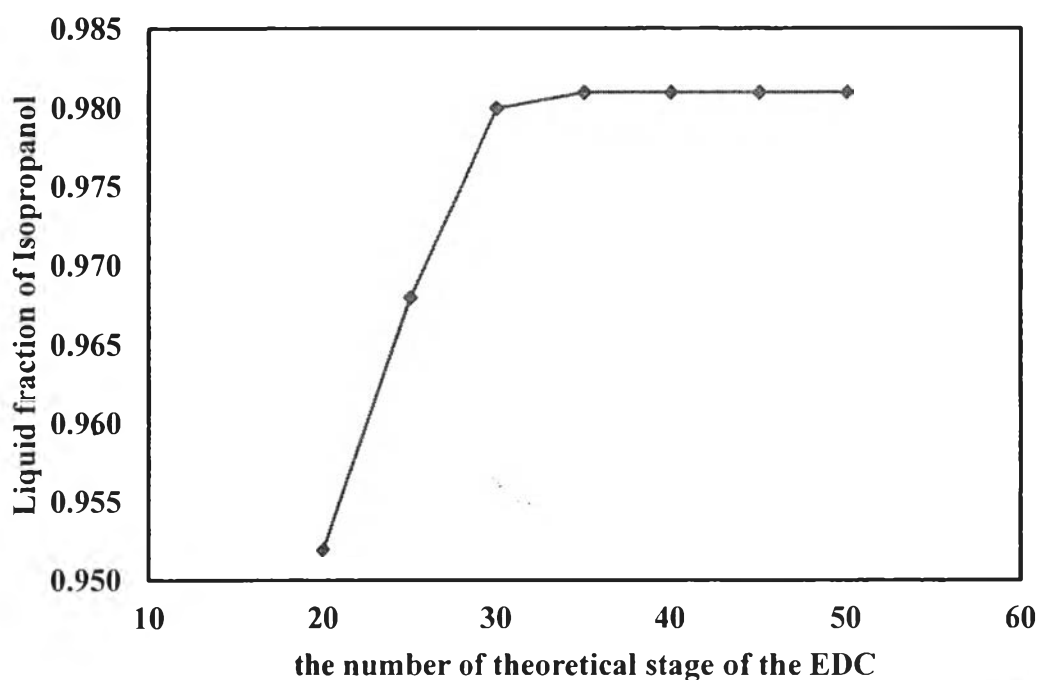


Figure 4.15 Comparison of the number of theoretical stage versus liquid molar fraction of the product (isopropanol) in extractive distillation using $[\text{C}_2\text{MIM}][\text{N}(\text{CN})_2]$.

Therefore, from the previous case of isopropanol + water separation using $[\text{C}_2\text{MIM}][\text{N}(\text{CN})_2]$ with 30 theoretical stages and RR of 0.729 was studied to observe the optimal theoretical stages. The simulation results are

displayed in Table 4.8. The theoretical stage of 26 was observed to recover isopropanol with a purity of 99.8 mol% at RR of 0.729. According to the results, the feed should be located at the 18th stage to obtain isopropanol with a molar purity of 0.998.

Table 4.8 The input variables and the theoretical stages results for isopropanol + water separation processes using [C₂MIM][N(CN)₂] when kept reflux ration as 0.729

	Isopropanol + water + [C ₂ MIM][N(CN) ₂]
Entrainer flow rate, kmol/h	120
Main column	
Theoretical stages	26
Operating pressure, kPa	100
Ethanol purity	99.8 mol %
Reflux ratio	0.729
Entrainer stage	2
Feed stage	18
Bottom temperature, °C	137.4
Reboiler heat duty, MW	2.54

4.2.4.2.3 The Change of the IL Flowrate in EDC

To compare the entrainer feed flowrate of the two azeotropic systems, the RR of 0.729 was fixed for the ethanol + water [C₂MIM][N(CN)₂] and isopropanol + water [C₂MIM][N(CN)₂] systems. The optimal results of both systems are presented in Table 4.8. A plot between the entrainer feed flowrate against the purity of isopropanol is presented in Figure 4.16. The optimal IL flowrates was observed at 120 kmol/hr for isopropanol + water system and 94 kmol/hr for the ethanol + water system to satisfy the design criterion of 0.998 mol% of distillate. Thus, an increase in size of the alcohol allows an increase in the IL feed

flowrate. The process simulation results of ethanol + water separation using $[C_2MIM][N(CN)_2]$ at $RR=0.729$ is presented in Figure D45 and Table D33.

Table 4.9 A comparison of the input variables and the theoretical stages results for isopropanol + water separation processes using $[C_2MIM][N(CN)_2]$ when kept reflux ration as 0.729

	Ethanol + water + $[C_2MIM][N(CN)_2]$	Isopropanol + water + $[C_2MIM][N(CN)_2]$
Entrainer flow rate, kmol/h	94	120
Main column		
Theoretical stages	30	30
Operating pressure, kPa	100	100
Distillate purity	99.8 mol %	99.8 mol %
Reflux ratio	0.729	0.729
Entrainer feed stage	2	2
Alcohol + water feed stage	22	22
Bottom temperature, °C	170	138.4
Reboiler heat duty, MW	3.36	2.54

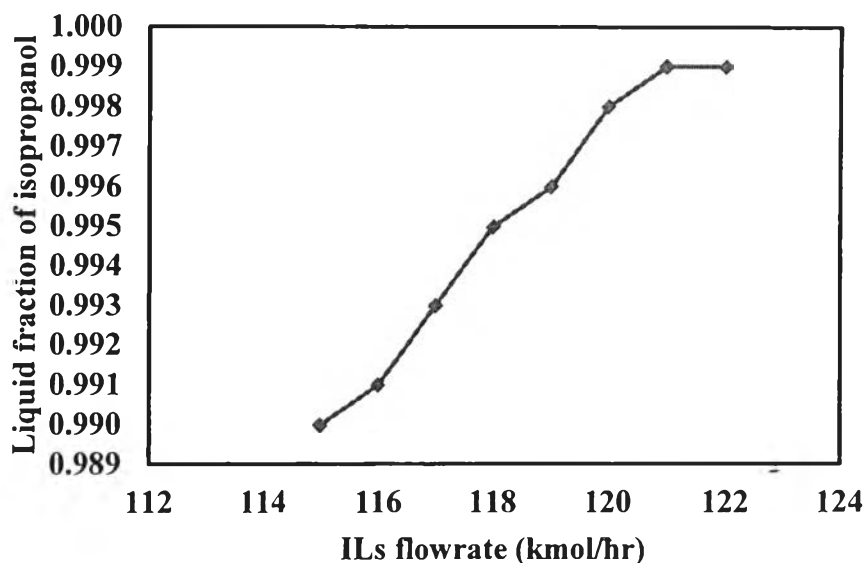


Figure 4.16 Comparison of the flowrate of $[\text{C}_2\text{MIM}][\text{N}(\text{CN})_2]$ versus liquid molar fraction of the isopropanol in EDC.

4.2.4.2.4 *The Change of the Temperature and the Heat Duty in Flash Drum*

The fixed parameters of the EDC for ethanol + water and isopropanol + water using $[\text{C}_2\text{MIM}][\text{N}(\text{CN})_2]$ are shown in Table 4.9. The pressure in the simple evaporation of the flash drum was set as 10 kPa, only the operating temperature and the heat duty were investigated by using optimizer (Pro/II 9.1). The flash simulation results of the isopropanol + water using $[\text{C}_2\text{MIM}][\text{N}(\text{CN})_2]$ are presented in Figure 4.17. The entrainer regeneration process required the operating temperature of 163 °C, and the flash heat duty of 1.12 MW. This required lower operating temperature than the ethanol + water separation process. In term of overall energy requirement, the separation of ethanol from the aqueous systems required energy of 4.13 MW, which was higher than the separation of isopropanol + water (3.66 MW) as shown in Figure 4.18. Thus, an increase of the size of the alcohol for the flash drum allows a decrease of the operating temperature, but an increase of the flash heat duty. However, the overall energy consumption of the whole process shows a decrease of 11.3 % as compared to that of the ethanol + water system.

Table 4.10 A comparison of the input variables and the theoretical stages results for isopropanol + water separation processes using $[\text{C}_2\text{MIM}][\text{N}(\text{CN})_2]$

	Ethanol + water + [C₂MIM][N(CN)₂]	Isopropanol + water + [C₂MIM][N(CN)₂]
Entrainer flow rate, kmol/h	120	120
Main column		
Theoretical stages	30	30
Operating pressure, kPa	100	100
Ethanol purity	99.8 mol %	99.8 mol %
Reflux ratio	0.729	0.729
Entrainer stage	2	2
Feed stage	22	22
Bottom temperature, °C	170	138.4
Reboiler heat duty, MW	3.51	2.54
Entrainer regeneration		
Entrainer purity	>99.8 mol %	>99.8 mol %
<i>Flash drum</i>		
Operating pressure, kPa	10	10
Operating temperature, C	200	163
Heat duty, MW	0.62	1.12
<i>Stripping column</i>		
Theoretical stages	10	10
Bottom temperature, °C	78	80
Air flow rate, kg/h	8071.1	8094
Air temperature, °C	25	25
Overall heat duty(Reboiler+Flash), MW	4.13	3.66

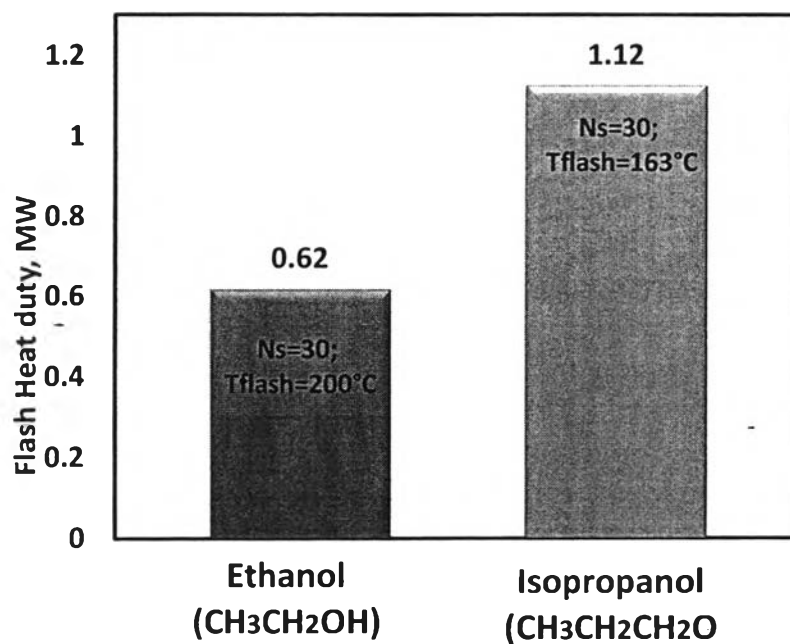


Figure 4.17 A comparison of the flash simulation results for the alcoholic aqueous azeotropic separation processes using [C₂MIM][N(CN)₂].

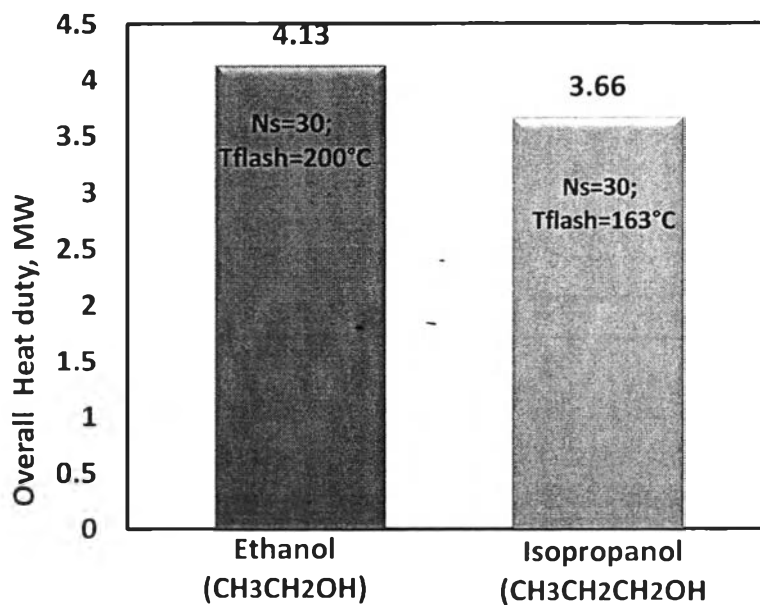


Figure 4.18 A comparison of the flash simulation results for the alcoholic aqueous azeotropic separation processes using [C₂MIM][N(CN)₂].

4.2.4.2.5 The Optimal Condition of the Isopropanol + Water Separation Using $[C_2MIM][N(CN)_2]$

The optimal column condition and the results of the isopropanol + water separation using $[C_2MIM][N(CN)_2]$ are summarized in Figure 4.19. The feed of the EDC is located at the 18th stage and the minimum number of stage of the EDC is 26. This EDC required the heat duty for reboiler of 2.54 MW and the heat duty for flash drum of 1.168 MW. The overall heat requirement of the whole process is 3.71 MW. The stream table results and column profiles of the whole processes can be seen in Table D36 and Figure D48-D51, respectively.

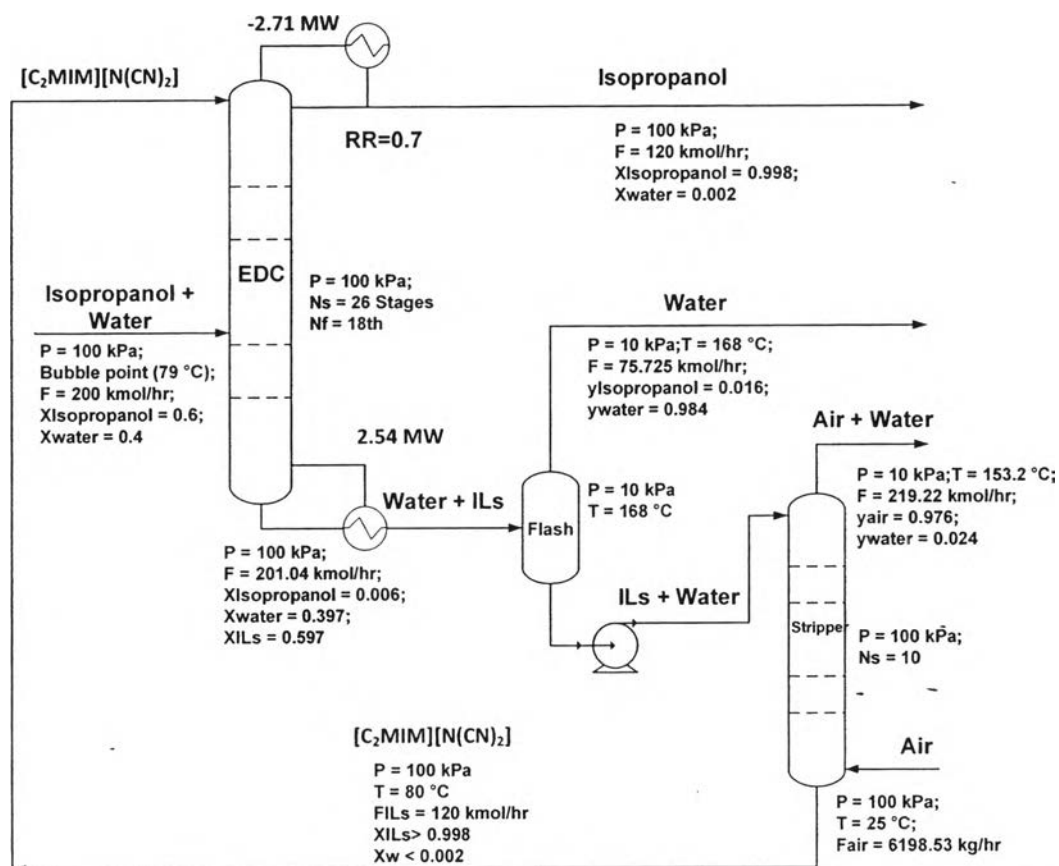


Figure 4.19 The optimal conditions and the results of the isopropanol + water azeotropic separation processes using $[C_2MIM][N(CN)_2]$.